

Molecular Dynamics Observations of Interdiffusion and Stranski-Krastanov Growth in the Early Film Deposition of Au on Ag(110)

Michael I. Haftel, Mervine Rosen, Tameika Franklin, and Matthew Hettermann

Code 6651, Naval Research Laboratory, Washington, D.C. 20375-5345

(Received 24 September 1993)

We simulate the vapor deposition of the first three monolayers of Au on Ag(110) with the molecular dynamics code DAMSEL using surface-embedded-atom potentials and utilizing simulated annealing. The simulations show interdiffusive Stranski-Krastanov growth, which is consistent with recent ion scattering and scanning tunneling microscopy studies. Most of the first deposited monolayer of Au burrows to the substrate layer, with further deposition leading to 3D growth resembling a 3×1 missing-row reconstruction. We discuss the dynamic mechanisms accounting for this growth.

PACS numbers: 68.35.Bs, 68.35.Ja, 68.55.Jk

A recent scanning tunneling microscopy (STM) analysis by Rousset *et al.* [1] indicates that the first monolayer of Au vapor deposited on Ag(110) at room temperature interdiffuses, or “burrows,” one layer below the surface, with the adlayer then consisting mostly of Ag atoms. While interdiffusion is not unknown in thin-film growth, it is quite unusual in metals especially for a heteroatomic system with a fairly small surface energy mismatch. On further deposition the STM analysis [1] suggests a burrowing of the first monolayer and subsequent 3D growth of “fingerlike” structures. This is a new, unusual modification of the Stranski-Krastanov (SK) growth mode. It contradicts an earlier interpretation [2] of medium energy ion scattering (MEIS) data, which indicated an early bilayer growth mode (with no interdiffusion), but the STM workers assert that their analysis [1] of the earlier MEIS data [2] is consistent with the interdiffusion picture.

Coincident with the STM experiments, Chan, Bohnen, and Ho [3] carried out total energy calculations of Au/Ag(110), with density functional theory, for various atomic layer configurations. They concluded that the energetically favored layered equilibrium configuration for 1 monolayer (ML) coverage is that in which the adlayer is completely covered by Ag with the Au “adatoms” occupying the layer just below this surface. Single or bilayer growth above the substrate is highly unfavorable. However, first-principles calculations presently cannot go beyond rather symmetric structures or a limited number of atoms. They cannot address the detailed dynamics of the deposition process or the formation of complicated structures.

In this paper we employ molecular dynamics (MD) simulations with semiempirical surface-embedded-atom method (SEAM) potentials [4,5] to model the film deposition of Au on Ag(110) up to 3 ML coverage. MD simulation allows us to mimic the experimental deposition process and to study in detail the growth and the dynamic processes that produce the atomic configurations for many different coverages.

The parameters of the SEAM potentials are fit to

single-crystal surface properties (surface energies, reconstructions of low index faces) as well as to bulk properties (as in the conventional EAM [6]). We will present the detailed parametrization for Ag and Au in a future work. We fit to the experimental values of the lattice constant, cohesive energy, and force constants for Au and Ag and also fit the surface energies for these metals [7]. In addition, the Au potential predicts quasihexagonal and missing-row reconstructions for the (100) and (110) faces, respectively, consistent with experiment [8–10]. Also consistent with experiment, the Ag potential predicts no reconstructions on these surfaces. The SEAM potentials have steeper embedding functions in the low electron density region relevant for the surface than do the EAM [11,12].

For Au/Ag growth we need to also specify an Au/Ag alloy potential. We take the form of the alloy pair potential from Ref. [5]:

$$V_{\text{Ag-Au}}(r) = 0.4V_{\text{Au}}(r) + 0.625V_{\text{Ag}}(r), \quad (1)$$

where the indicated arithmetic weighting of potentials gives the best fits to the heats of solution of Au in Ag and the reverse (-0.138 and -0.147 eV, respectively, compared to -0.19 and -0.16 eV experimental [13]). The renormalization of electron densities discussed in Ref. [5] turns out to be unnecessary for this particular alloy potential.

We simulate deposition by computationally annealing [5] the system, integrating generalized Langevin equations of motion, under constant-volume-constant-temperature periodic boundary conditions, with the molecular dynamics code DAMSEL [14]. Atoms are deposited, one (or a few) at a time, onto $6\times 8\times 17$ unit cells, with each adatom placed above the surface just within the force range of its nearest surface atom. The initial temperature for each deposition is taken sufficiently high (about 850 K) so that significant surface diffusion can occur over MD time scales (≤ 1 ns). Then the system is cooled to 0 K over ~ 1 ns. For coverages > 0.5 ML we deposit the atoms one at a time at a constant temperature with about 50 ps between depositions, then cool to 0 K

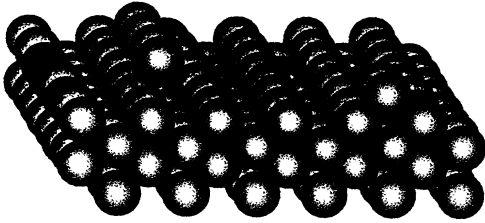


FIG. 1. Atomic configuration after 6 Au atoms have been deposited on a 6×8 Ag(110) substrate (0.125 ML coverage). The light atoms are Ag; the dark atoms Au.

after half monolayer intervals. These procedures mimic room-temperature vapor deposition in that the elevated temperature allows the atoms to sample a good deal of phase space and overcome activation barriers for surface diffusion. The slow cooling and deposition rates [over ≤ 1 ns, which is still orders of magnitude faster than laboratory time scales for room-temperature deposition (over seconds to hours)] allow the atoms to seek kinetically accessible equilibrium positions as they would at room temperature. [The distinction between 0 K and room temperature is not important in this regard. Our simulations indicate that at room temperature, over MD time scales (~ 1 ns), all atoms just undergo small amplitude oscillations around the equilibrium positions without surmounting any activation barriers.]

Figures 1–3 illustrate the atomic configurations after the deposition of 6, 24, and 48 Au atoms, respectively, on the 6×8 Ag substrate, corresponding to 0.125, 0.5, and 1.0 ML coverages. In Fig. 1 the adlayer consists of 6 Ag atoms, with all of the Au atoms sinking to the substrate layers. While the atomic replacement (or “exchange”) is responsible for the absorption of the Ag into the substrate, the rather high mobility of Ag on Ag(110) allows some “unshadowing” of the Au.

At 0.5 ML (Fig. 2) a “burrowing,” or interdiffusion, of Ag below the surface shows up quite clearly. The burrowed Au on the first substrate layer are fairly evenly dispersed.

At 1 ML coverage (Fig. 3) the adlayer contains 15 of the 48 deposited Au atoms, with about 75% of the bur-

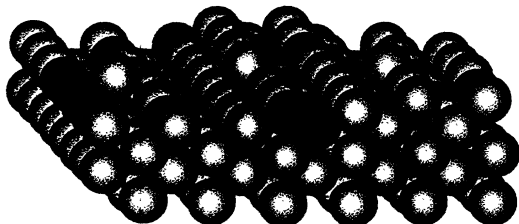


FIG. 2. Atomic configuration for 24 Au atoms deposited on Ag(110) (0.5 ML).

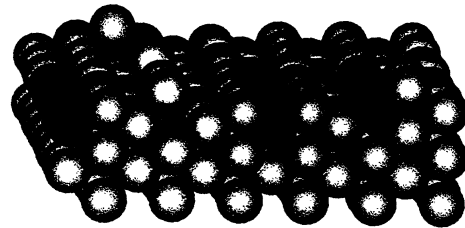


FIG. 3. Atomic configuration for 48 Au atoms deposited on Ag(110) (1.0 ML).

rowed atoms on the top substrate layer. Overall, to this point the growth is mainly layer by layer. This fits the STM observation [1] of the absence of islanding at 1 ML.

Figure 4 (3.0 ML coverage) illustrates a 3D growth after the deposition of the first monolayer. The prominent 3D structure on the right-hand side is essentially the 3×1 missing-row reconstruction characterized by elongated islanding in the $[1\bar{1}0]$ direction. (The extent of the MD cell—six atomic spacings in the $[100]$ direction—is the minimum for which a 3×1 missing-row reconstruction could show up at all, but is probably too small to observe this reconstruction as a regular pattern.) This feature is conceivably the genesis of the 3D “finger” growth in this direction observed in STM experiments [1]. As the deposition continued from 1 to 3 ML, Ag atoms occupy a decreasing portion of the exposed surface on which to exchange with incident Au atoms and hence a slowing of interdiffusion.

We expect the system to seek the energetically favorable configurations as long as they are kinetically accessible. Chan, Bohnen, and Ho [3] found that alloying one layer below the surface is most favorable for 0.5 ML coverage and complete interdiffusion of Au at 1 ML, while single-layer growth was favorable over bilayer growth for the first monolayer above the surface. Our molecular statics calculations using the SEAM potential, summarized in Table I, yield the same trends. The table, which gives the heats of formation per Au atom for various “ideal” structures, includes results for the Foiles-Daw-

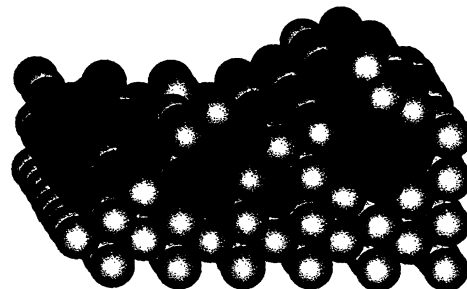


FIG. 4. Atomic configuration for 144 Au atoms deposited on Ag(110) (3.0 ML).

TABLE I. Heats of formation (in eV per Au atom) of relaxed ideal configurations predicted by SEAM, the EAM of Foiles, Baskes, and Daw (FDB) [11], and the density functional (DF) calculation of Chan, Bohnen, and Ho [3]. Our definition of the heat of formation is the negative of that used by Chan, Bohnen, and Ho. The alloy configuration assumes $c(2 \times 2)$ coverage for each element.

Configuration	SEAM	FDB	DF
1 Au in Ag bulk	-0.13770	-0.10828	?
1 Au layer on top	0.04356	0.06697	-0.122
2 Au layers on top	0.05143	0.04770	-0.050
1 Au layer below 1 Ag layer	-0.14298	-0.06682	-0.26
1 Au layer below 2 Ag layers	-0.12291	-0.09027	-0.21
1 alloy layer below 1 Ag layer	-0.16592	-0.08449	-0.30

Baskes (FDB) EAM potential [11] as well. Both SEAM and the density functional calculations of Chan, Bohnen, and Ho indicate the following: (1) 1 ML coverage on the surface; FDB favors bilayer. (2) The most favorable growth for 1 ML coverage is for one Au layer to burrow beneath one layer of Ag; FDB prefers one Au layer to burrow beneath two layers of Ag. (3) The most energetically favorable configuration considered is for there to be an Au-Ag alloy layer beneath one layer of Ag; such an alloy layer is not favored by FDB. (A constant shift between the heats of formation predicted by SEAM, FDB, and Chan, Bohnen, and Ho could be accounted for by different heats of solution of a single Au in bulk Ag. This quantity is not given in Ref. [3].)

As suggested by Fig. 1, the most probable dynamic processes are atomic replacement [15] of Au adatoms with substrate Ag, and surface hopping of Ag atoms. The former process largely accounts for the interdiffusion of Au, but the latter allows some unshadowing of substrate Au atoms. Some of the subsequent deposited Au fall on top of unshadowed Au atoms, where they are relatively immobile and begin a 3D "pileup." Since surface diffusion of Ag is somewhat less probable (per atom) than the replacement by Au, the burrowing proceeds for a good fraction of a monolayer before 3D growth eventually takes over.

To confirm this view, we carried out a separate simulation of the simultaneous deposition of three Au atoms onto a Ag(110) substrate. In this simulation we heated the system from 0 to 1400 K over 600 ps. We found that the Au-Ag replacements started to occur at 400 K, and surface hopping of Ag (along $[1\bar{1}0]$ nearest-neighbor rows) at about 500 K. This implies low activation barriers for these two processes (probably < 0.1 eV), but with the barrier for replacement lower. Ag-Ag replacements began at ~ 750 K. Other processes—such as Ag-Au or Au-Au replacement, Ag or Au hopping other than in nearest-neighbor rows, and certain "opportunistic" processes [16]—showed up rather infrequently (for $T < 800$ K) and would not play a large role. A similar

simulation carried out with the FDB potential yields a higher threshold for Au-Ag replacement at ~ 600 K, and this is preceded by Au surface hopping at ~ 500 K. While most Au atoms did eventually "burrow" (five out of the first six) with the FDB potential, they have less of a tendency to do this than with the SEAM potential.

Our MD simulations of Au on Ag(110) confirms the interdiffusive mode of SK growth for this system as indicated by the STM experiments. A preliminary analysis of the MD results for the shadowing effect for normal incidence ion scattering yields reductions in the Ag and Au yields similar to those measured in the MEIS experiments. The interdiffusion is initiated by the easy atomic replacement of Ag substrate atoms by the incident Au atoms with the absorption of the Au into the substrate. However, a fraction of the substrate Au atoms become exposed because of the high surface mobility of Ag, and 3D growth begins to become the coping mechanism for lowering the surface energy. In the SEAM calculation the 3D growth is similar in structure to the 3×1 missing-row reconstruction of Au(110), which was suggested in the MEIS experiments, and consistent with the fingerlike growth in the $[1\bar{1}0]$ direction observed in the STM images.

The atomic replacement mechanism [15] is at the heart of the burrowing phenomenon of the early growth of Au on Ag(110). The SEAM potentials have steep embedding functions (to better fit surface energies) and consequently emphasize bond saturation features of the interatomic force and hence favor high coordination on the surface [17]. This same feature leads to the quasihexagonal reconstructions of Au and Pt(100) as well as to the desirability of the replacement mechanism during deposition. The replacement process should be more efficient than surface "hopping" in maximizing the atomic coordination during deposition. This is especially true for Au, which has a higher surface energy and a steeper embedding function than Ag, and a quasihexagonal (100) reconstruction. The SEAM results for Au/Ag(110) increase the confidence of using the SEAM approach in predictions of early film growth features for metal-on-metal systems. We are currently investigating the early stages of film growth for other homoepitaxial and heteroepitaxial metallic systems using this approach.

The authors thank Dr. Leonard Feldman for helpful discussions.

-
- [1] S. Rousset, S. Chiang, D. E. Fowler, and D. D. Chambliss, Phys. Rev. Lett. **69**, 3200 (1992).
 - [2] P. Fenter and T. Gustafsson, Phys. Rev. Lett. **64**, 1142 (1990); Phys. Rev. B **43**, 12195 (1991).
 - [3] C. T. Chan, K.-P. Bohnen, and K. M. Ho, Phys. Rev. Lett. **69**, 1672 (1992); K.-P. Bohnen, C. T. Chan, and K. M. Ho, Surf. Sci. Lett. **268**, L284 (1992).

- [4] M. I. Haftel, *Mater. Res. Soc. Proc.* **238**, 229 (1992).
- [5] Michael I. Haftel, *Phys. Rev. B* **48**, 2611 (1993).
- [6] M. S. Daw and M. I. Baskes, *Phys. Rev. Lett.* **50**, 1285 (1983); *Phys. Rev. B* **29**, 6443 (1984).
- [7] W. R. Tyson and W. A. Miller, *Surf. Sci.* **62**, 267 (1977).
- [8] M. A. Van Hove *et al.*, *Surf. Sci.* **103**, 189 (1981); **103**, 218 (1981).
- [9] Q. J. Gao and T. T. Tsong, *Phys. Rev. B* **36**, 2547 (1987).
- [10] C. M. Chan and M. A. Van Hove, *Surf. Sci.* **171**, 226 (1986); E. Vlieg, I. K. Robinson, and K. Kern, *Surf. Sci.* **233**, 248 (1990).
- [11] S. M. Foiles, M. I. Baskes, and M. S. Daw, *Phys. Rev. B* **33**, 7983 (1986).
- [12] D. J. Oh and R. A. Johnson, *J. Mater. Res.* **3**, 471 (1988).
- [13] R. Hultgren, P. D. Desai, D. T. Hawkins, M. Gleiser, and K. K. Kelley, *Selected Values of the Thermodynamic Properties of Binary Alloys* (American Society for Metals, Metals Park, OH, 1973).
- [14] M. I. Haftel, T. D. Andreadis, J. V. Lill, and J. M. Eridon, *Phys. Rev. B* **42**, 11 540 (1990).
- [15] P. A. Feibelman, *Phys. Rev. Lett.* **65**, 729 (1990).
- [16] J. E. Black and Zeng-Ju Tian (to be published).
- [17] This feature of the embedding function and its relation to effective two- and three-body potentials is discussed in detail in Ref. [5]. The discussion there points out that if the embedding function is defined by requiring it to have a minimum at the bulk equilibrium bulk electron density, then this function exhibits entirely the quadratic energy price one pays in any departure from bulklike coordination. (Only a linear price is paid from the residual pair potential.)

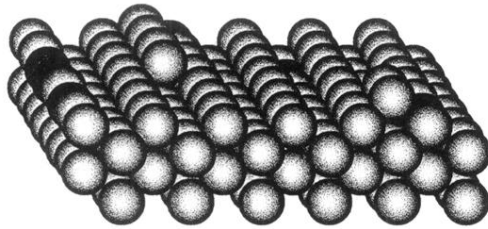


FIG. 1. Atomic configuration after 6 Au atoms have been deposited on a 6×8 Ag(110) substrate (0.125 ML coverage). The light atoms are Ag; the dark atoms Au.

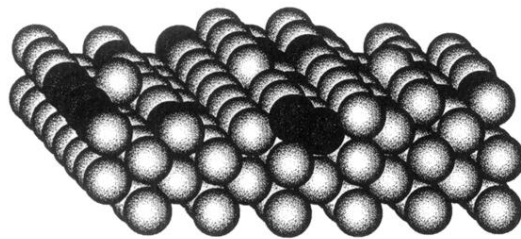


FIG. 2. Atomic configuration for 24 Au atoms deposited on Ag(110) (0.5 ML).

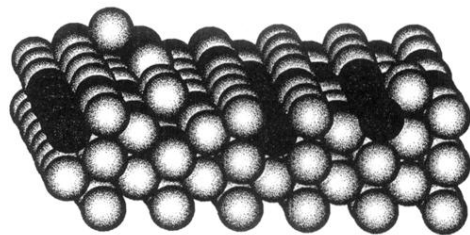


FIG. 3. Atomic configuration for 48 Au atoms deposited on Ag(110) (1.0 ML).

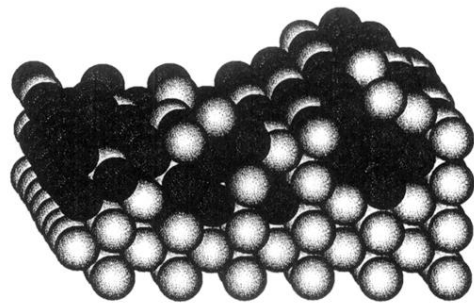


FIG. 4. Atomic configuration for 144 Au atoms deposited on Ag(110) (3.0 ML).